Title
Binding Kinetic Rates Measured via Electrophoretic Band Crossing in a Pseudohomogeneous Format

Journal
Analytical Chemistry, 86(5)

ISSN
0003-2700

Authors
Kapil, Monica A
Herr, Amy E

Publication Date
2014-03-04

DOI
10.1021/ac403829z

Peer reviewed

analytical chemistry

Article

pubs.acs.org/ac

Binding Kinetic Rates Measured via Electrophoretic Band Crossing in a Pseudohomogeneous Format

Monica A. Kapil and Amy E. Herr*

Department of Bioengineering, University of California, Berkeley, California, 94706, United States

Supporting Information

ABSTRACT: With relevance spanning from immunohistochemistry to immunoassays and therapeutics, antibody reagents play critical roles in the life sciences, clinical chemistry, and clinical medicine. Nevertheless, nonspecific interactions and performance reproducibility remain problematic. Consequently, scalable and efficient analytical tools for informed selection of reliable antibody reagents would have wide impact. Therefore, we introduce a kinetic polyacrylamide gel electrophoresis (KPAGE) microfluidic assay that directly measures antibody–antigen association and dissociation rate constants, k_{on} and k_{off}. To study antibody–antigen association, an antigen zone is electrophoresed through a zone of immobilized antibody. Upon crossing, the interaction yields a zone of immobilized immunocomplex. To quantify k_{on}, we assess immunocomplex formation for a range of antigen–antibody interaction times. Here, interaction time is controlled by the velocity of the electromigrating antigen zone, which is determined by the strength of the applied electric field. All species are fluorescently labeled. To quantify k_{off}, an immobilized zone of immunocomplex is subjected to in situ buffer dilution, while measuring the decay in immunocomplex concentration. Two approaches for antibody immobilization are detailed: (i) size-exclusion-based antibody immobilization via a molecular weight cutoff (MWCO) filter fabricated using polyacrylamide gel and (ii) covalent antibody immobilization realized using a photoactive benzophenone methacrylamide polyacrylamide gel. We determine k_{on} and k_{off} for prostate-specific antigen (PSA) and compare to gold-standard values. The KPAGE assay completes in 90 min, requiring 45 ng of often-limited antibody material, thus offering a quantitative antibody screening platform relevant to important but difficult to characterize interaction kinetics.

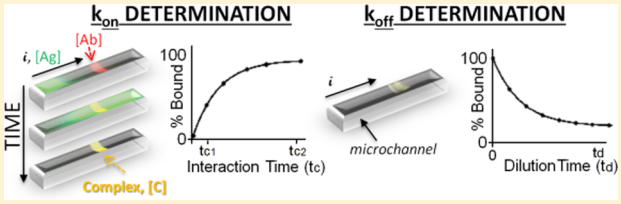

For assays that rely on antibody-based detection, selection of an antibody reagent presents a critical challenge.[1,2] Nonspecific binding and reproducibility remain problematic.[1,3,4] Typical immunoreagent selection criteria include affinity determination for an antibody–antigen interaction quantified by the equilibrium constant (K_d). The K_d describes the dynamic equilibrium between association (binding) and dissociation (unbinding). Although K_d is widely used for antibody selection[5,6]—and can be related to kinetic association and dissociation rate constants (k_{on} and k_{off})—the direct measurement of k_{on} and k_{off} provides more specific information on binding and dissociation, both of which are useful as selection criteria.[7−9] In other words, two antibodies with identical K_d values may have dramatically different binding kinetics, making performance for a specific application difficult to predict. For example, identification of an antibody–antigen pair possessing a high association rate but low dissociation rate will result in appreciable binding with persisting immunocomplex, as may be desired in immunohistochemistry. Such considerations are also important in assays that involve advection or diffusion (e.g., washing or incubation steps, separation steps).

Gold standard immunoreagent screening and selection assays, such as enzyme-linked immunosorbent assays (ELISAs) and surface plasmon resonance (SPR) do not report both k_{on} and k_{off} directly,[5,10] yielding instead a measurement of K_d. In ELISA, an antigen is immobilized to a solid surface (96-well plate) and then complexed with an antibody linked to an enzyme. Through a series of equilibrium experiments, the K_d can be quantified; however, these measurements rarely yield values reflecting reliable equilibrium constants due to mass transport limitations.[11] These mass transport limitations increase the time needed for the antibody to reach the immobilized antigen. The time and concentrations needed for the reaction to reach equilibrium are often unknown and underestimated. In fact, the reaction may never reach equilibrium, thus ELISA provides a qualitative measurement of relative binding, rather than a quantitative assessment.[12,13] In addition, ELISA is time-consuming, taking 4 h up to overnight to come to equilibrium allowing extraction of the K_d.

Like ELISA, SPR facilitates the measurement of K_d via label-free detection of antigen binding to chemically surface-immobilized antibodies by detecting refractive index changes at the binding surface. Due to the heterogeneous SPR format and the poorly defined surface density of the immobilized antibody, SPR cannot make direct measurement of k_{on}.[14] However, k_{on} can be calculated via the relationship: $k_{on} = k_{off}/$

Received: November 26, 2013
Accepted: February 10, 2014
Published: February 10, 2014

   dx.doi.org/10.1021/ac403829z | Anal. Chem. 2014, 86, 2601−2609

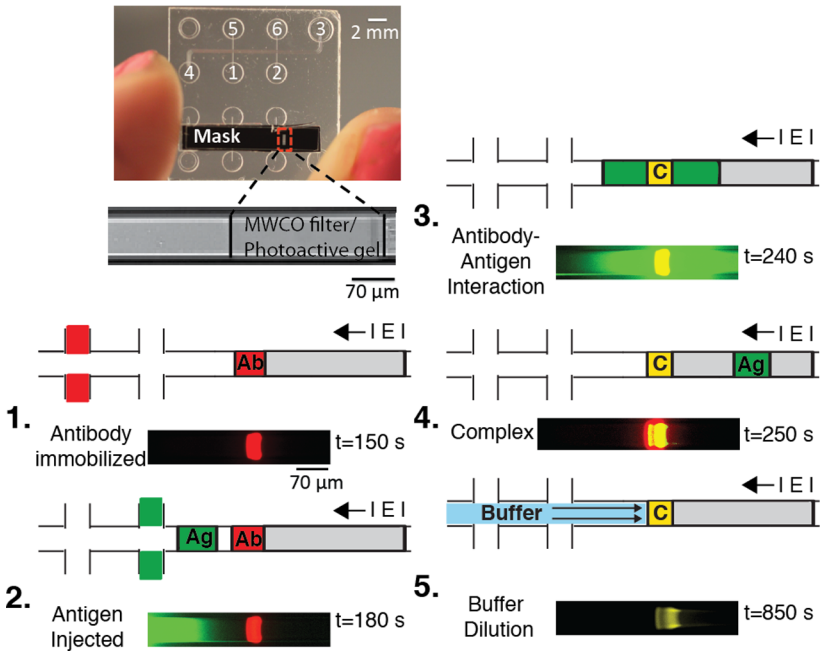

Figure 1. Direct measurement of binding kinetic constants k_{on} and k_{off} via KPAGE relies on an immobilized antibody zone and a freely electromigrating antigen zone. The microchannel assay is composed of five steps: (Step 1) antibody (Ab) immobilization (MWCO filter and photoactive gel methods), (Step 2) antigen (Ag) sample injection, (Step 3) antibody–antigen interaction, (Step 4) complex (C) formation, and (Step 5) buffer dilution where the "|E|" for each step represents the direction of the electric field.

K_d, when k_{off} is known. Further SPR measurement limitations stem from challenges in supplying sufficient analyte transport to the sensor surface and chemical immobilization of the antibody.[14] Both factors hinder binding and introduce mass transport limitations.[15−18] Consequently, 10−100× slower direct measurements of k_{on} values are reported in comparison to SPR calculated k_{on} values.[19] Finally, the SPR immobilization procedure can be time-consuming, labor-intensive, and expensive.[20]

Kinetic capillary electrophoresis (KCE) is a powerful alternate technique for making direct measurements of k_{on} and k_{off}.[21−24] In plug−plug kinetic capillary electrophoresis (ppKCE) short plugs (zones) of antigen and antibody are injected into a 20−40 cm long capillary. The sample zone with the lower mobility is injected first, followed by injection of the high mobility species. During the assay, the trailing species zone overruns the slower leading species zone. As both species are in solution, the assay benefits from reaction characteristics of a homogeneous (not heterogeneous) format, thus eliminating concerns associated with concentration depletion boundary layers that can form in heterogeneous reactions. The overspeeding duration sets the interaction time and yields formation of a third species zone, the immunocomplex. The immunocomplex subsequently resolves from the two reactant zones. Both k_{on} and k_{off} are calculated from a single ppKCE electropherogram using the area of the peak, signal "tailing" and "fronting", and migration time scales. Owing to high separation efficiency, fast speed, and minute sample consumption, KCE has been intensively studied for measurement of the binding constants and binding stoichiometry of various affinity interactions.[25−27] Although kinetic capillary electrophoresis methods do not require the surface immobilization needed for SPR and ELISA, measurements of k_{on} and k_{off} require fairly complex and iterative mathematical manipulations of resultant electropherograms and, of course, sufficient mobility difference between species zones for reasonable resolution of the formed complex and free antigen.[28]

Taken together, characterization of antibody reagents in a rapid, facile, and low-reagent-consuming format suitable for screening would have wide impact. Here, we introduce an electrophoretic microfluidic assay, termed kinetic polyacrylamide gel electrophoresis (KPAGE), which directly quantifies both association and dissociation rates, k_{on} and k_{off}, and the dissociation constant K_d. Association is determined by observing a fluorescently labeled antigen zone electromigrate through an immobilized antibody zone. The k_{off} is quantified by observing dissociation of immunocomplex as clear buffer (i.e., antigen not present) is electrophoresed through the antibody-immobilized zone of immunocomplex. Two approaches to in situ antibody immobilization are investigated, including immobilization of an antibody zone at a microscale size exclusion filter (step change in pore size) and covalent immobilization of an antibody zone on a photoactive polyacrylamide gel (uniform pore size). Using both approaches, we apply the KPAGE assay to study of a well-validated system of prostate-specific antigen (PSA) and a cognate monoclonal antibody. Results suggest this low-infrastructure microfluidic KPAGE assay is a feasible means to realize rapid, quantitative, and scalable antibody screening tools, without the need for complex data interpretation or immobilization schemes.

MATERIALS AND METHODS

Apparatus and Imaging. Fluorescence images were collected using an inverted epi-fluorescence microscope equipped with CCD camera, filter cubes, and an automated $x-y$ stage. The CCD exposure time was 10−100 ms depending on the intensity of the fluorescence signal. Image analysis was conducted using ImageJ software (NIH, Bethesda, MD). (See Supporting Information, Methods for more information on imaging systems used.)

dx.doi.org/10.1021/ac403829z | Anal. Chem. 2014, 86, 2601−2609

Reagents. Silane, glacial acetic acid, methanol, acrylamide, bis-acrylamide, and the chemical initiators, such as ammonium persulfate (APS) and tetramethylethylenediamine (TEMED) were all purchased from Sigma-Aldrich. UV photoinitiator was purchased from Wako Chemicals. A 10× Tris/glycine native electrophoresis buffer (25 mM Tris, 192 mM glycine, pH 8.3) was purchased from Bio-Rad. Benzophenone methacrylamide monomer (BPMA, (*N*-[3-[(4-benzoylphenyl) formamido]-propyl] methacrylamide) was synthesized and characterized by PharamAgra Laboratories, Inc. Proteins and antibodies were fluorescently labeled in-house using Alexa Fluor 488 and 568 protein labeling kits from Invitrogen and purified by Bio-Gel columns from Bio-Rad. Purified prostate-specific antigen (PSA) and Anti-Prostate Specific Antigen antibody were purchased from Abcam. Alexa Fluor 568 Goat Anti-Mouse IgG (H+L) antibody was purchased from Life Technologies Corporation. (See Supporting Information, Methods for more information on reagents used.)

Chip Preparation. Glass microfluidic chips with double cross T-junction channels were designed in-house using AutoCAD 2012. Three parallel channels, each with a depth of 20 μm and a width of 70 μm were fabricated using a standard wet etching[29] process (Caliper Life Sciences, Hopkinton, MA). Chip surface preparation prior to gel polymerization was performed as described previously.[30] Two fabrication approaches were developed for realizing an immobilized zone of antibody.

Immobilization Approach 1: Size-Exclusion Antibody Immobilization via a Molecular Weight Cutoff (MWCO) Filter. The MWCO filter was fabricated using a two-step mask-based photopolymerization process as described previously[30] using a precursor solution of 10% *T* (*T*, the concentration of total acrylamide, w/v), 5.5% *C* (*C*, ratio of bisacrylamide and bisacrylamide + acrylamide, w/w) for the filter and 3% *T*, 3.3% *C* for the loading gel. For more details see Supporting Information, Methods. After use, polyacrylamide was removed from the microchannel network (allowing glass chip reuse) by soaking the chips in a 2:1 solution of 70% perchloric acid and 30% hydrogen peroxide overnight at 60 °C, as described previously.[31] Proper precautions should be carefully observed.

To conduct KPAGE using the MWCO filter, 10 μL of 1× Tris/glycine or protein sample diluted in Tris/glycine was added to channel termini reservoirs (i.e., pipet tip press-fit into the termini wells). In step (1) Figure 1, antibody (Ab, 20nM) was electrophoretically loaded from the top T-junction (wells 1 and 5), and a plug of Ab was injected and immobilized at the MWCO filter (wells 4 and 3), by physical exclusion of large molecular mass Ab at the filter pore-size discontinuity (interface). Owing to the physical exclusion from the filter, the local Ab concentration enriched 5× (100nM ± 20%). In step (2), a plug of antigen (Ag) (10 uM) was electrophoretically loaded at the bottom T-junction (wells 2 and 6) and electrophoretically injected into the reaction channel (wells 4 and 3). The applied potential was adjusted to control the band-crossing interaction time (t_c) allowing interactions times in the range 1 s < t_c < 60 s. So, to obtain different interaction times, the electric field is adjusted. Different field strengths should yield different channel transit times for each antigen zone, thus the peak width and maximum concentration of the antigen zone should be different upon arrival at the immobilized antibody zone (Supporting Information, Figure S-1). Consequently, to expose each immobilized Ab zone to a similar antigen plug concentration, regardless of t_c, we implemented a two-step injection process. First, antigen was injected and electrophoresed to the 1 mm point at a high *E*. Second, upon reaching the 1 mm mark, *E* was decreased to provide the desired t_c. The maximum antigen concentration was 7 μM ± 500nM. In step (3), epi-fluorescence micrographs were collected continually at the immobilized Ab zone enabling monitoring of the immunocomplex formation and direct measurement of the electric field-controlled t_c. To reset the assay in step (4), after immunocomplex (C) measurement was made, field polarity was reversed across the filter to electrophorese away C, Ab, and Ag. Steps (1) through (4) were repeated for the series of t_c. In step (5), to determine the dissociation rate constant, equilibrium mixtures of C were incubated overnight. A plug of C was electrophoretically loaded to wells 2 and 6 and injected into the MWCO filter (wells 4 and 3). The complex was subjected to buffer dilution for a dilution time (t_d) of 60 min while monitored via epi-fluorescence imaging. (See Supporting Information, Methods for more information on the fabrication and voltage protocol used.)

Immobilization Approach 2: Covalent Antibody Immobilization via a Photoactive Polyacrylamide Gel. The photoactive polyacrylamide gel was fabricated using a precursor solution of 4% *T*, 3.3% *C*. BPMA monomer was added to precursor solutions at 1.1 mM from a 100 mM stock in DMSO. Gels were chemically initiated by 0.08% each of APS and TEMED in a buffer of 1× Tris/glycine. Degassed precursor was introduced to channels by capillary action. Precursor (4 μL) was added to each well. To avoid diffusion of oxygen into the channel and thus inhibition of acrylamide polymerization, a cover glass slide was placed on top of the glass chips to cap the wells at the channel termini. Chips were incubated for ∼10 min until gelation of excess precursor on top of the chip was observed.

To conduct KPAGE using the photoactive gel immobilization method, we developed a protocol similar to the MWCO filter method; the major difference is the method of Ab immobilization. In Approach 2, covalent attachment of Ab to the benzophenone containing polyacrylamide gel through UV photopatterning was used, not physical exclusion as in the MWCO in Approach 1. To immobilize a plug of Ab (step 1), Ab (2 μM) was first loaded into the reaction channel (wells 4 and 3). A photomask with a 20 μm slit was designed and fabricated in-house. The slit was cut in stainless steel using a laser cutter (Universal Laser Systems, PLS6MW Multi-Wavelength Laser Platform (30W fiber laser cartridge) (Scottsdale, AZ)). The mask was placed on top of the glass chip, with the slit 1 mm downstream from the second double cross T-junction. Flood UV (350−365 nm) light was provided by a Hamamatsu Lightningcure LC5 directed through a liquid light guide (Newport Corporation, 77566 Liquid Light Guide) for 5 s at 20% intensity. Contact masking was used, with the liquid light guide pressed directly onto the mask surface. After UV exposure, electrophoresis was resumed to remove free Ab from the channel (wells 4 and 3). The Ab capture efficiency was defined as the fraction of antibody that was retained in the channel after UV exposure and washout to the antibody initially loaded into the channel before UV exposure. UV capture efficiencies depend on the benzophenone concentration within the gel, UV exposure times, and the amount of available C−H bonds in target polypeptides and proteins. In addition, we have observed sample preparation to be an important factor in binding efficiency of protein to gel scaffold. For example, we

dx.doi.org/10.1021/ac403829z | *Anal. Chem.* 2014, 86, 2601−2609

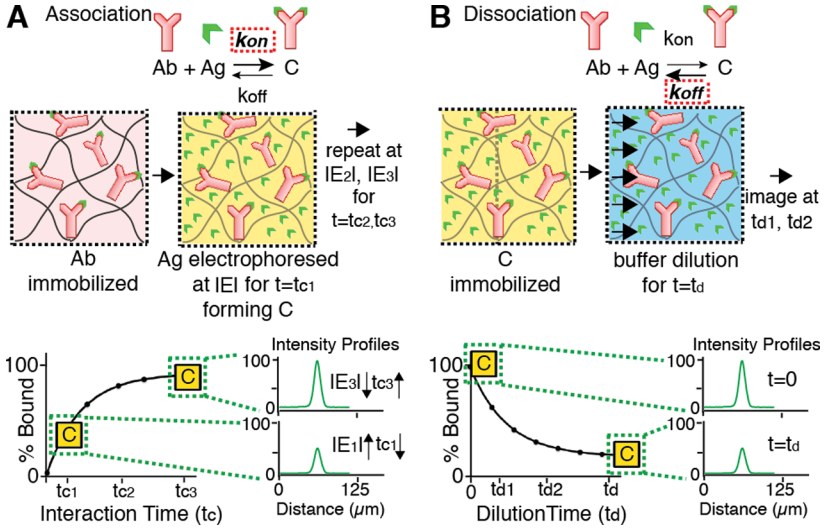

Figure 2. KPAGE schemes for determination of both association and dissociation rate constants. (A) Association rate determination: A zone of antibody (Ab) is immobilized in a polyacrylamide gel. A plug of fluorescently labeled antigen (Ag) is electrophoresed through the stationary antibody for a set interaction time (t_c). Sufficient interaction time results in formation of stationary immune complex (C). By sweeping through a range of t_c experiments, the amount of complex formed for each condition allows estimation of k_{on}. Here, t_c is varied by controlling the electrophoretic velocity of the antigen through the applied electric field, E. (B) Dissociation rate determination: A plug of immunocomplex is immobilized in the polyacrylamide gel and buffer is swept over the complex for a set dilution time, t_d. The time-dependent decay in the complex signal allows determination of k_{off}.

have observed native proteins to immobilize with notably less efficiency (1.5%, under IEF conditions)[32] than fully reduced/denatured proteins (>85%).[33] In line with the native protein immobilization efficiencies previously observed, KPAGE reports antibody capture efficiencies of 8.8% ± 2%. Steps (2−4) follow the MWCO filter method as described above. For step (5), Ab was immobilized as stated in step (1) and antigen was electrophoretically loaded through the reaction channel (wells 4 and 3) until the complex reached equilibrium. The complex was then subjected to buffer dilution via electrophoresis for a t_d of 60 min, with imaging conducted every 10 min using a 100 ms exposure time. Replicates were performed using a new channel and photoimmobilized plug of antibody for each interaction and dilution. After loading and photocapture of antibody, residual background signal was observed with an SNR >3.3.

Fluorescence Signal Calibration. To quantify the local antigen and antibody concentrations, calibration curves were generated, and photobleaching studies were conducted. (See Supporting Information, methods).

Estimation of Interaction Time, t_c. For k_{on} measurements, the t_c was defined as the time required for a zone of antigen (at a known concentration) to traverse the zone of immobilized Ab. As fluorescent antigen electromigrated through the immobilized Ab zone, fluorescence signal was collected and integrated from the Ab region (axial length of 10−170 μm, transverse width of 70 μm) as a function of time. This capture region was designed such that we could obtain interaction times before the reaction reached equilibrium, as discussed in the Results and Discussion section. The signal was fitted to Gaussian distributions numerically (MATLAB R2010b), with the full width at half-maximum (fwhm) computed and used as the t_c. The antigen distributions used to determine t_c were asymmetrical for the MWCO filter as the immobilized Ab region was located at the sharp MWCO filter interface. As antigen enters the immobilized Ab region, the zone enters a small pore size gel and slows, accelerating again when the zone exits the filter into a higher pore size gel. Antibody−antigen interaction times were controlled by varying the electric fields from 1739 V/cm to 38 V/cm yielding analyte velocities from 500−10 μm/s and interaction times from 2 to 60 s, with standard deviations for each interaction time up to 0.25 s for a given applied field.

Estimation of Kinetic Rate Constants k_{on} and k_{off}. Epifluorescence micrographs of the immobilized Ab and (bound antigen) immunocomplex signals for each t_c and t_d were fitted to Gaussian distributions numerically (MATLAB R2010b). The area under the curve (AUC) of the antibody and immunocomplex signal was determined by integrating the Gaussian distribution. The antibody and immunocomplex concentration in (nM) was obtained using calibration curves developed as described above. For k_{on} measurements, the percent bound (% Bound) for each immunocomplex concentration was computed by taking the ratio of the immunocomplex to available binding sites, % Bound = C/Ab. For each interaction time, a control was performed to determine the amount of nonspecific binding occurring at the filter interface. This value was subtracted before quantifying the immunocomplex concentrations for a given interaction time. We employ a Langmuirian one-to-one antibody-to-antigen binding model.[7] We chose this model, because monoclonal antibody purification is known to result in protein unfolding, misfolding, and aggregation that may yield only one active binding site.[34,35] Experimental data was fit to the binding association and dissociation expressions.[36]

Transport Modeling. We numerically modeled the antibody, antigen, and immunocomplex concentration for a series of time points for the KPAGE assay. (See Supporting Information, Methods.)

RESULTS AND DISCUSSION

KPAGE Assay Design. To yield an efficient, scalable, and readily interpretable assay for determination of antibody−antigen kinetic rate constants, we explored a purely electro-

dx.doi.org/10.1021/ac403829z | Anal. Chem. 2014, 86, 2601−2609

phoretic pseudohomogeneous band-crossing format, as described in the Materials and Methods and briefly summarized here (Figure 2). During KPAGE k_{on} determination, a zone of fluorescently labeled antigen was electrophoresed through an immobilized zone of antibody for a known and controlled interaction time, t_c. Given sufficient t_c, electromigrating antigen binds to the immobilized antibody forming a stationary immunocomplex. Note that either antibody or antigen can be immobilized in the photoactive KPAGE system but only the larger of the binding pair can be immobilized for the MWCO filter method, both with the mobile analyte in excess. Several crossing experiments with distinct t_c durations were performed, each using a zone of fresh immobilized antibody. Increasing or decreasing the t_c was controlled by varying the electrophoretic velocity of the antigen through adjustment of the applied electric field strength. At longer t_c, the amount of immunocomplex formed is higher (until equilibrium), with the amount of resultant immunocomplex directly related to k_{on} of the binding pair. To determine the dissociation rate, a zone of pre-equilibrated antigen−antibody immunocomplex was immobilized in the microchannel. Buffer was electrophoresed over the stationary immunocomplex for a set dilution time (t_d), and the decay in immunocomplex concentration was monitored. KPAGE offers a pseudohomogeneous format that is reaction-limited, with mass transport of free antigen to immobilized antibody fast in comparison to the reaction, owing to small diffusional lengths (100 nm) defined by the porous gel matrix.

In designing the KPAGE assay, we first sought to determine the types of binding pairs well-suited for KPAGE analysis. We simulate the KPAGE assay and then consider assay requirements for three binding rate regimes: low, intermediate, and ultrahigh (Figure 3A). The simulations estimate the range of association and dissociation rates using a 1D diffusion, convection, and reaction model. The parameter that dictates the KPAGE-accessible range for the association and dissociation rates depends on the electrophoretic velocity of the antigen, which controls the interaction time. The electrophoretic velocity of the antigen zone through the antibody capture zone is the same for both the MWCO filter and photoactive gel methods, and hence this model predicts the accessible regimes irrespective of the exact immobilization method employed. For k_{on}, KPAGE must allow ∼4 measurements of immunocomplex formation before equilibrium is reached.[36] With the equilibrium time given by $\tau_{eq} = (k_{on}Ag + k_{off})^{-1}$, this criterion can be stated as: $t_c < (\tau_{eq}/4)$. An example of a low association rate constant system[37] is free PSA and a monoclonal antibody with a $k_{on} = 4.1 \times 10^4$ M^{-1} s^{-1}. For an intermediate system,[37−39,12,15] a $k_{on} = 4.0 \times 10^6$ M^{-1} s^{-1} is appropriate. For an ultrahigh[40] affinity binding pair such as biotin and streptavidin, a $k_{on} = 4.5 \times 10^7$ M^{-1} s^{-1} is appropriate. For low and intermediate association rates, the τ_{eq} was found to be within 10 s < τ_{eq} < 20 s. Given $t_c < \tau_{eq}$, we assume negligible dissociation. Using an electromigration−diffusion−reaction model, we estimate the fastest interaction time attainable as ∼1 s. Thus, the KPAGE association assay must be capable of measuring ∼4 distinct t_c values in the first 10 s. Although this analysis suggests that assay operation is not well-suited to ultrafast binding pairs (i.e., streptavidin−biotin), the analysis does suggest that KPAGE is well-suited to a wide range of antibody−antigen binding pairs (e.g., 1.0×10^4 M^{-1} $s^{-1} \leq k_{on} \leq 1.0 \times 10^6$ M^{-1} s^{-1}), including those of interest in this work.

Similarly, for dissociation kinetic rate constant or k_{off} determination, we simulated a range of binding pairs (Figure 3B): one pair with a low dissociation rate (e.g., biotin[40] and streptavidin with $k_{off} = 7.5 \times 10^{-8}$ s^{-1}), one with an intermediate dissociation rate (e.g., PSA[41] with $k_{off} = 4.5 \times 10^{-5}$ s^{-1}), and one pair with a high dissociation rate (e.g., human serum albumin and ketoprofen[42] with $k_{off} = 0.227$ s^{-1}). In the limiting case of low k_{off} (Figure 3B), the simulation predicts a dilution time of 1 h, yielding a minimal decrease in complex signal, by AUC determination. In fact, a dilution time of 7 weeks would reduce the AUC of the immunocomplex by just 5%, which is the minimum signal decrease needed to reliably compute k_{off} via KPAGE. Nevertheless, for typical antibody−antigen pairs, simulation results predict the majority of immunocomplex dissociating within 1 h of dilution initiation, making dissociation readily measurable using KPAGE. Finally, simulation of high k_{off} systems predicts that the immunocomplex AUC should diminish notably within just the first 30 s of dilution.

Next, we sought to understand the applicability of KPAGE to measurement of k_{off}. For this analysis, we assume that newly dissociated and now electromigrating antigen (free antigen) does not reassociate with immobilized Ab during the assay duration. To scrutinize this assumption, we compare an "on-time" (t_{on}) and an "off-time" (t_{off}) representative of KPAGE. Assuming antigen is in surplus, we define t_{on} as the time required for antigen to bind with an antibody and form immunocomplex. Thus, t_{on} can be related to the antibody concentration, Ab, and the association rate, k_{on}, yielding $t_{on} = (k_{on}\ Ab)^{-1}$. We further define t_{off} as the immobilized antibody zone length, L, divided by the antigen electromigration velocity, uAg, yielding $t_{off} = L(u_{Ag})^{-1}$. Under KPAGE operating conditions and intermediate association rate kinetics, comparison suggests that the time needed for antigen to electromigrate past the immobilized antibody zone is substantially lower than

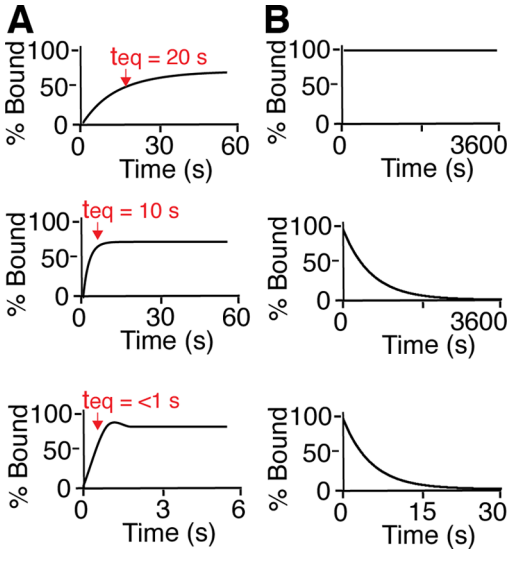

Figure 3. Binding kinetic regime simulations inform KPAGE applicability. (A) Association kinetic rate constants in three association rate regimes: low, intermediate, and ultrahigh. As association kinetic rate increases, the time to equilibrium decreases from 20 s to <1 s. (B) Dissociation kinetic rate constants in three dissociation rate regimes: low, intermediate, and high. Low dissociation kinetic rates require unrealistic KPAGE measurement durations, whereas intermediate and high dissociation rates are measurable via KPAGE.

dx.doi.org/10.1021/ac403829z | Anal. Chem. 2014, 86, 2601−2609

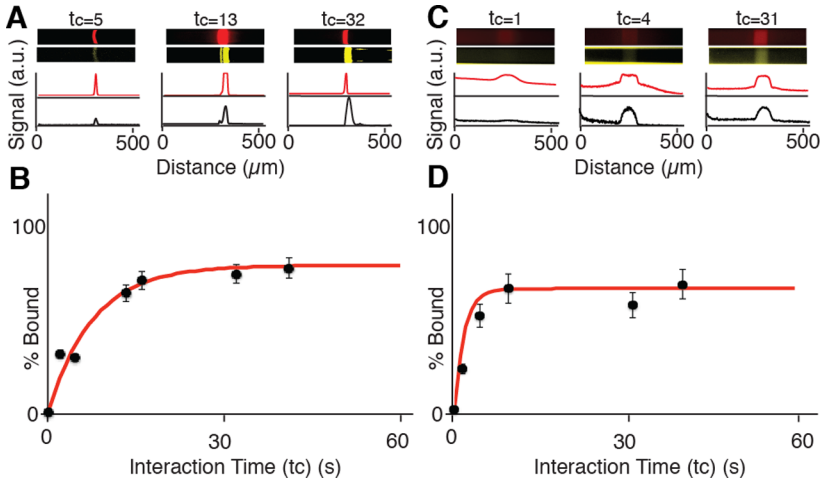

Figure 4. Direct determination of association rate constants with KPAGE. Two-color epi-fluorescence micrographs of immunocomplex (merged red and green fluorophore signals) formed after antigen (green fluorophore) has interacted with the immobilized antibody (red fluorophore) for a set interaction time, t_c. The MWCO filter antibody immobilization method (left panel) and the photoactive gel antibody immobilization method (right panel) are both shown. (A,C) Intensity profiles of immune complex peaks at different interaction times (t_c) points ranging from 0−60 s are quantified and shows that as t_c increases, the AUC of the immune complex peaks increases. (B,D) On-chip measurements of the association rate constant k_{on} were calculated from a three-parameter binding curve fit model (red) and plotted against the measured PSA immune complex % Bound for each t_c. Error bars are calculated from three replicate trials. The k_{on} for the affinity interaction of PSA was 2×10^4 M^{-1} s^{-1} ± 7% for the MWCO filter method (left) and 2.7×10^5 M^{-1} s^{-1} ± 12% for the photoactive gel method (right).

the time needed for antigen to bind to antibody ($t_{off} \ll t_{on}$). For example, for KPAGE with t_{off} = 0.1 and t_{on} = 10, at analyte velocities as fast as 500 μm s^{-1} with antibody capture zones of 10−170 μm in axial length, dissociated antigen exits the immobilized antibody zone before rebinding with immobilized antibody. An upper limit on electric potential sourced by the high voltage power supply used for KPAGE limits the maximum electrophoretic velocity of the antigen zone.

KPAGE Determination of Association Kinetic Rate Constant, k_{on}. We applied KPAGE to determine k_{on} of a PSA and monoclonal antibody pair. First, we used a polyacrylamide MWCO filter to facilitate size exclusion and thus immobilization of antibody at the filter interface (Figure 4A). We observed the (axial) length of the immobilized antibody zone ranging from 10 to 70 μm (n = 12 devices) with ∼50% variation in the total mass of antibody immobilized, as determined by AUC measurements. As such, t_c was explicitly measured for each run from image sequences acquired during the band-crossing experiments. We observed immunocomplex signal increasing with longer t_c durations, as expected for $t_c < \tau_{eq}$. As shown in Figure 4B, binding curves plateau at 64% of the antigen bound in immunocomplex, with the asymptote value dependent on concentration of antigen and immobilized antibody. Interestingly, although the electromigrating PSA concentration was ∼60 times greater than that of the immobilized antibody, we did not observe saturation of the immobilized antibody under any t_c studied. We attribute this reduced binding occupancy (even at long interaction times) to possible steric hindrance of antibody binding sites owing to crowding at the MWCO filter interface[30] or due to high dissociation rates.

In light of the size-exclusion-based immobilization mechanism used to determine k_{on}, we sought to further understand the role of nonspecific adsorption of free protein, as the MWCO filter excludes species based on size. To characterize sources of nonspecific binding at the MWCO filter, we explored performance in four different cases: (Case 1) KPAGE with no antibody present, (Case 2) KPAGE with an immobilized off-target antibody (goat antimouse IgG (H + L)), (Case 3) KPAGE with PSA-specific antibody immobilized, and (Case 4) KPAGE with no polyacrylamide gel pore-size discontinuity and no immobilized antibody zone (i.e., uniform, bare gel). For each case, a high concentration zone of PSA antigen (10 μM) was electrophoresed across the region of interest, and any signal retained was quantified by calculating the AUC.

With no antibody present (Case 1), we measured a 23 ± 2% nonspecific signal for the MWCO filter immobilization method. With off-target antibody immobilized at the MWCO filter (Case 2), we measured a 20 ± 4% nonspecific signal. A uniform pore size bare gel (Case 4) yielded no detectable signal. All of these cases were then compared to signal from immobilized on-target PSA antibody (Case 3), where we measured an AUC signal 5-fold greater than Cases 1 and 2. Taken together, we attribute nonspecific signal to the presence of the pore-size discontinuity that forms the MWCO filter. As such, background signal correction was performed for each KPAGE measurement conducted using a MWCO filter, to account for any antigen nonselectively trapped at the pore-size discontinuity.

For the PSA and monoclonal antibody pair, MWCO-filter-based KPAGE reported a k_{on} value of 2.0×10^4 M^{-1} s^{-1} ± 7% (n = 3, Figure 3B). In comparison, SPR determination of k_{on} for the PSA monoclonal antibody pair[41] has been reported as 4.1×10^4 M^{-1} s^{-1} ± 25%, thus showing appreciable agreement with KPAGE using the MWCO filter. When considering SPR, we note that this surface-based assay is known to be mass transport limited under a range of operating conditions. When operating in a mass-transport-limited mode, the binding reaction at the surface consumes free antigen faster than mass transport (diffusion, convection) can deliver fresh, unbound antigen to the surface. The development of a depletion boundary layer in free antigen concentration proximal to the surface causes SPR to report ∼10−100× lower association kinetic rate constants when measured directly.[19] Although a pseudohomogeneous system such as KPAGE overcomes the k_{on} artifacts arising from concentration depletion boundary layers, our observations of the KPAGE system further suggest that local crowding of antibody at the filter interface may lead to a reduced ability for

dx.doi.org/10.1021/ac403829z | Anal. Chem. 2014, 86, 2601−2609

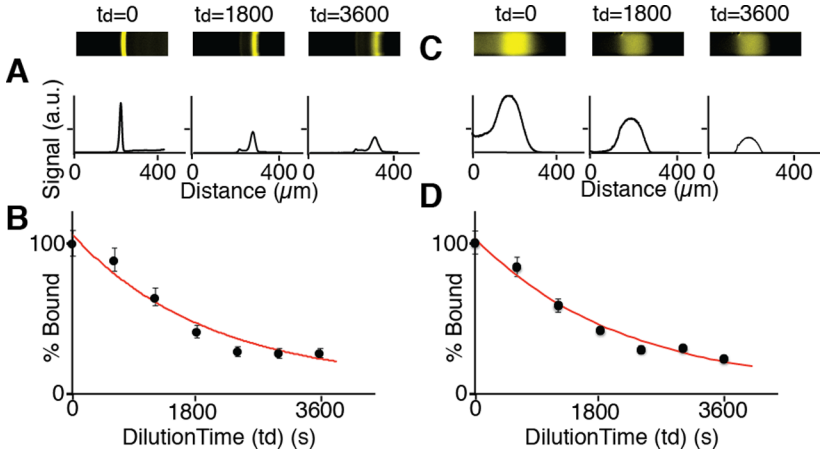

Figure 5. Direct determination of dissociation rate constants via KPAGE. Two-color epi-fluorescence micrograph time course of PSA immunocomplex dissociation (C, merged red and green fluorophore signals). The MWCO filter antibody immobilization method (left panel) and the photoactive gel antibody immobilization method (right panel) are shown (A,C). Intensity profiles of immune complex peaks at different dilution times (t_d) points ranging from 0 to 3600 s are quantified. As t_d increases, the AUC of the immune complex peaks decreases. (B,D) Black circles represent on-chip measurements of PSA immune complex % Bound at different t_d. On-chip measurements of the dissociation rate constant k_{off} was calculated from a three-parameter binding curve fit model (red) and plotted against the measured PSA immune complex % Bound for each t_c. Error bars are calculated from replicate trials. The k_{off} was determined to be 5.0×10^{-4} s^{-1} ± 7.5% for the MWCO filter method (left) and 4.7×10^{-4} s^{-1} ± 7.2% for the photoactive gel method (right).

the immobilized antibody to bind to antigen owing to crowding artifacts (i.e., steric hindrance or epitope masking), as mentioned.

We next explored alternate means to locally immobilize antibody while overcoming the challenges of antibody crowding and nonspecific interactions with the MWCO filter. As a second approach to immobilizing antibody, we utilized a polyacrylamide gel containing benzophenone methacrylamide monomer. This "photoactive" formulation allows UV-initiated covalent immobilization of a zone of antibody to the polyacrylamide gel through hydrogen abstraction (Figure 4C). In contrast to the MWCO filter immobilization approach, mask-based photopatterning of antibody allows use of a uniform pore size polyacrylamide gel and relaxes the size-based assay design constraints. The antibody zone lengths ranged from 80 to 170 μm.

Importantly, we performed a study of nonspecific interactions using the same set of control studies examined for the MWCO filter immobilization approach. Here, we measured a 3.8 ± 0.2% nonspecific signal for Case 1, a 3.5 ± 0.3% nonspecific signal for Case 2. In a uniform pore size, bare gel (Case 4), no detectable signal was measured. All cases were then compared to signal from immobilized on-target PSA antibody (Case 3), where we measured a signal 33-fold greater than Cases 1 and 2. As an aside, we observed notably less variation in the run-to-run antibody mass loaded (8%) when using the photoactive gel as compared to the MWCO filter approach. We attribute tighter control of antibody immobilization to the uniform pore size of the gel and, hence, similar electrical resistance of all fabricated microchannels (i.e., reduced chip-to-chip variation). Recall that protein and antibody are loaded into the gels electrophoretically.

After observing notably reduced nonspecific interactions as compared to the MWCO filter approach, k_{on} for the PSA and monoclonal antibody pair was determined (Figure 4C). KPAGE with covalently immobilized antibody estimated a k_{on} of 2.7×10^5 M^{-1} s^{-1} ± 12% (n = 3, Figure 4D) for the PSA and antibody pair. Like the MWCO filter method, the photoactive gel method sees a binding curve that plateaus at 64% of the antigen bound in immunocomplex. Saturation of the immobilized antibody did not occur, even at long interaction times. We attribute the observed plateauing behavior to high antibody concentrations and dissociation rates. In comparison, SPR can yield run-to-run calculation-based k_{on} variation near 25%,[16,41,43] thus suggesting KPAGE is more robust than SPR.

Compared to the MWCO filter and SPR, the association kinetic rate constant measured for PSA and monoclonal antibody is an order of magnitude faster in the photoactive gel system. Further, the equilibration time is 3× faster than the equilibration time observed using the KPAGE MWCO filter approach (15 s). We hypothesize that the differences in observed kinetic characteristics stem from differences in the physical environment and mechanism underpinning antibody immobilization. First, we note that the KPAGE system was operated under pH 8.3 buffer conditions to support electrophoresis, whereas the SPR studies cited were performed in a pH 7.4 buffer as is typical of SPR. The local pH influences the protein state and, therefore, electrostatic interactions and overall binding. Previous reports have observed that, as the pH increases, the association rates of antibody−antigen pairs can increase by as much as 85%,[44] and dissociation rates can increase by as much as 16-fold.[45,46] In a study comparing an IgG antibody to an enzymatic protein similar to PSA, hen egg lysozyme (HEL), association rate increased by 33% when increasing the pH by just one unit (pH 7 to pH 8). Comparing PSA SPR results to our KPAGE results, we observed a 70% increase in association rates. These results follow the trend previously published[44] and are in range of what is to be expected when increasing the pH of the run buffer for this type of antibody−antigen pair. Second, for the MWCO filter, pore sizes at the filter interface are smaller than the antibody, allowing the antibody to be immobilized based on size exclusion. As antigen plug is electrophoresed through the immobilized antibody zone at varying electric field strengths, the antibody zone is observed to further electromigrate into the gel (up to ∼25 μm past the filter interface) and widen by 50%

dx.doi.org/10.1021/ac403829z | Anal. Chem. 2014, 86, 2601−2609

(n = 3) (see Supporting Information, Figure S-3). This localized concentration reduction and embedded nature of the immobilization potentially limits accessibility of epitope binding sites. In contrast, the photoactive gel immobilization approach yields stationary covalent attachment of the antibody to a uniform pore size gel matrix.

KPAGE Determination of Dissociation Kinetic Rate Constant, k_{off}, and Computed K_d. We next applied KPAGE to measure the dissociation rate constant of the PSA and monoclonal PSA antibody pair, here again comparing the MWCO filter (Figure 5A,B) and photoactive gel immobilization approaches (Figure 5C,D). For both approaches, we observed time-dependent dissociation of immunocomplex, asymptoting to 20−30% at the longest dissociation times studied (i.e., 3600 s). KPAGE yielded two measurements for k_{off}, with the MWCO filter reporting 5.0×10^{-4} s^{-1} ± 7.5% and the photoactive gel reporting 4.7×10^{-4} s^{-1} ± 7.2%. Despite the differences in the physical environment and immobilization mechanism of both the MWCO filter method and the photoactive gel method, both methods yield similar k_{off} values. We hypothesize that despite steric hindrance or epitope masking that could be occurring in the MWCO filter method, once complex is formed, dissociation of the antigen upon buffer dilution occurs at the same rate as the photoactive gel. This type of behavior has been previously observed in a similar study,[47] which compared two types of antibody immobilization methods, that is, (1) a three-dimensional hydrogel-binding matrix (1 μm in thickness) to (2) a dextran matrix (100 nm thickness). In this study, the association rate for the hydrogel-binding matrix was an order of magnitude lower than the dextran matrix;[37] however, for the dissociation rates, both methods were similar. The dissociation constant K_d computed from k_{off} and k_{on} for the MWCO filter and photoactive gel methods were 25 and 1.7 nM. Taken together, KPAGE by either immobilization method yields consistent k_{off} and K_d values. Literature reports based on SPR[41] establish k_{off} for PSA as 4.5×10^{-5} s^{-1} ± 15%, and computed dissociation rate constants of K_d = 1.86 nM. The k_{off} from SPR is roughly an order of magnitude lower than k_{off} determined by KPAGE and is the same order of magnitude for the computed K_d. Kinetic capillary electrophoresis determination of K_d values are comparable to SPR.[21,48] We hypothesize that differences in the measured values stem from differences in the pH of the binding system.

KPAGE Comparison: Molecular Weight Cutoff (MWCO) Filter Method and the Photoactive Gel Method. The MWCO filter method and photoactive gel method will each find use under specific assay constraints. The MWCO filter method should be employed (1) when binding partners in a pair differ considerably in molecular mass and (2) to immobilize the larger of two binding partners. Even with this rigid constraint, the MWCO filter is well-suited for measuring antibody−antigen interactions under native conditions (i.e., no covalent attachment) or for hydrophobic species. On this latter point, after exposure of the photoactive gel to UV, the gel becomes hydrophobic[33,49] and exhibits notable nonspecific interactions (lectins, carbohydrate-binding proteins),[50] a phenomenon not observed with the MWCO filter. The photoactive gel is well-suited to study the binding between analytes of similar molecular mass. Both immobilization methods use electrophoresis to introduce analyte into the channels and, therefore, buffers used will need to support electrophoresis. The majority of proteins in their native state have isoelectric points below 7.5, and a typical buffer used for electrophoresis will have a pH of 8−9. In addition, for the MWCO filter method, the gels can be reused up to 20 times by reversing the field and clearing out the complex in the filter with clear buffer. However, with the photoactive gels, the gels are limited to a single use. For both methods, after use the polyacrylamide gels can be removed from the microchannel network and chips reused with new gels. Both the MWCO filter and photoactive gel methods were designed for adoption by well-equipped biology laboratories. In addition to microdevices, standard equipment and reagents (e.g., epi-fluorescence microscopes, polyacrylamide gel precursors) are required.

CONCLUSIONS

Here, we report on the design, development, optimization, and characterization of KPAGE, a rapid, quantitative microfluidic-binding assay for direct quantification of kinetic rates for immunoreagent selection and quality assessment. We characterize each of two different methods of antibody immobilization: immobilization via a MWCO filter (where antibody is immobilized via size exclusion at a gel pore-size interface) and immobilization via a photoactive gel (where antibody is covalently attached to a polyacrylamide gel matrix via masking and UV exposure). A major KPAGE design consideration is fulfilled by allowing for pseudohomogeneous reaction conditions, as compared to transport-limited heterogeneous systems such as SPR. Empirical and numerical analyses of the KPAGE assay were performed and suggest that this system is well-suited to measure a wide range of antibody−antigen binding pairs with association rates ranging from 1.0×10^4 M^{-1} s^{-1} to 1.0×10^6 M^{-1} s^{-1} and dissociation rates that range from $k_{off} = 4.5 \times 10^{-5}$ s^{-1} to 2.7×10^{-1} s^{-1} to ultrahigh dissociating pairs such as human serum albumin and ketoprofen. Characterization of k_{on} and k_{off} was performed for the well-characterized and widely reported PSA−monoclonal antibody pair. This low-infrastructure KPAGE assay provides a feasible means to realize rapid, quantitative, antibody screening, without the need for complex data interpretation or immobilization schemes. We see KPAGE as a potentially powerful binding screening assay to assess important but difficult to characterize interaction kinetics, such as protein−protein and protein−DNA.

ASSOCIATED CONTENT

Supporting Information

Additional information as noted in the text. This material is available free of charge via the Internet at http://pubs.acs.org.

AUTHOR INFORMATION

Corresponding Author

*E-mail: aeh@berkeley.edu. Fax: 520-642-5835. Tel.: 510-666-3396.

Notes

The authors declare no competing financial interest.

ACKNOWLEDGMENTS

The authors acknowledge members and alumni of the Herr Lab for helpful discussion and critical feedback, as well as the QB3 Biomolecular Nanofabrication Center (BNC) for infrastructure. The authors gratefully acknowledge Dr. Albert P. Pisano and Dr. Jim C. Cheng from the Department of Mechanical Engineering at UC Berkeley for providing infrastructure and expertise in fabricating the stainless steel photomask. M.A.K. is

a National Science Foundation (NSF) Graduate Research Fellow. This work was supported by a National Science Foundation CAREER award (CBET-1056035 to A.E.H.). A.E.H. is an Alfred P. Sloan research fellow in chemistry.

REFERENCES

(1) Brennan, D. J.; O'Connor, D. P.; Rexhepaj, E.; Ponten, F.; Gallagher, W. M. *Nat. Rev. Cancer* **2010**, *10*, 605−617.
(2) Lilja, H.; Ulmert, D.; Vickers, A. J. *Nat. Rev. Cancer* **2008**, *8*, 268−278.
(3) Carlsson, A.; Wingren, C.; Ingvarsson, J.; Ellmark, P.; Baldertorp, B.; Fernö, M.; Olsson, H.; Borrebaeck, C. A. K. *Eur. J. Cancer* **2008**, *44*, 472−480.
(4) Wu, A. R.; Kawahara, T. L. A.; Rapicavoli, N. A.; Riggelen, J. v.; Shroff, E. H.; Xu, L.; Felsher, D. W.; Chang, H. Y.; Quake, S. R. *Lab Chip* **2012**, *12*, 2190−2198.
(5) Friguet, B.; Chaffotte, A. F.; Djavadi-Ohaniance, L.; Goldberg, M. E. *J. Immunol. Methods* **1985**, *77*, 305−319.
(6) Hawkins, R. E.; Russell, S. J.; Winter, G. *J. Mol. Biol.* **1992**, *226*, 889−896.
(7) Karlsson, R.; Michaelsson, A.; Mattsson, L. *J. Immunol. Methods* **1991**, *145*, 229−240.
(8) Malmborg, A. C.; Michaelsson, A.; Ohlin, M.; Jansson, B.; Borrebaeck, C. A. *Scand. J. Immunol.* **1992**, *35*, 643−650.
(9) Dandliker, W. B.; Levison, S. A. *IHC* **1968**, *5*, 171−183.
(10) Malmqvist, M. *Curr. Opin. Immunol.* **1993**, *5*, 282−286.
(11) Nygren, H.; Stenberg, M. *J. Colloid Interface Sci.* **1985**, *107*, 560−566.
(12) Hardy, F.; Djavadi-Ohaniance, L.; Goldberg, M. E. *J Immunol Methods* **1997**, *200*, 155−159.
(13) Karlsson, R.; Falt, A. *J. Immunol. Methods* **1997**, *200*, 121−133.
(14) van der Merwe, P. A. In *Protein−Ligand Interactions: Hydrodynamics and Calorimetry*; Harding, S. E., Chowdry, B. Z., Eds.; Oxford University Press: Oxford, U.K., 2001; pp 137−170.
(15) Nieba, L.; Krebber, A.; Pluckthun, A. *Anal. Biochem.* **1996**, *234*, 155−165.
(16) Myszka, D. G.; Morton, T. A.; Doyle, M. L.; Chaiken, I. M. *Biophys. Chem.* **1997**, *64*, 127−137.
(17) van der Merwe, P. A.; Bodian, D. L.; Daenke, S.; Linsley, P.; Davis, S. J. *J. Exp. Med.* **1997**, *185*, 393−404.
(18) Schuck, P. *Annu. Rev. Biophys. Biomol. Struct.* **1997**, *26*, 541−566.
(19) de Mol, N. J.; Plomp, E.; Fischer, M. J.; Ruijtenbeek, R. *Anal. Biochem.* **2000**, *279*, 61−70.
(20) Spisak, S.; Tulassay, Z.; Molnar, B.; Guttman, A. *Electrophoresis* **2007**, *28*, 4261−4273.
(21) Heegaard, N. H.; Olsen, D. T.; Larsen, K. L. *J. Chromatogr. A* **1996**, *744*, 285−294.
(22) Okhonin, V.; Petrov, A. P.; Berezovski, M.; Krylov, S. N. *Anal. Chem.* **2006**, *78*, 4803−4810.
(23) Petrov, A.; Okhonin, V.; Berezovski, M.; Krylov, S. N. *J. Am. Chem. Soc.* **2005**, *127*, 17104−17110.
(24) Jiang, C.; Armstrong, D. W. *Electrophoresis* **2010**, *31*, 17−27.
(25) Xiong, C.; Xia, Z.; Huang, R.; Chen, H.; Xu, P. *Sci. China, Ser. B: Chem.* **2008**, *51*, 1087−1092.
(26) Bao, J.; Krylova, S. M.; Reinstein, O.; Johnson, P. E.; Krylov, S. N. *Anal. Chem.* **2011**, *83*, 8387−8390.
(27) Drabovich, A.; Berezovski, M.; Krylov, S. N. *J. Am. Chem. Soc.* **2005**, *127*, 11224−11225.
(28) Krylov, S. N. *Electrophoresis* **2007**, *28*, 69−88.
(29) Bousse, L.; Mouradian, S.; Minalla, A.; Yee, H.; Williams, K.; Dubrow, R. *Anal. Chem.* **2001**, *73*, 1207−1212.
(30) Apori, A. A.; Herr, A. E. *Anal. Chem.* **2011**, *83*, 2691−2698.
(31) He, M.; Herr, A. E. *Nat. Protoc.* **2010**, *5*, 1844−1856.
(32) Tia, S. Q.; Brown, K.; Chen, D.; Herr, A. E. *Anal. Chem.* **2013**, *85*, 2882−2890.
(33) Hughes, A. J.; Lin, R. K.; Peehl, D. M.; Herr, A. E. *Proc. Natl. Acad. Sci. U.S.A.* **2012**, *109*, 5972−5977.
(34) Bilgiçer, B. a.; Thomas, S. W.; Shaw, B. F.; Kaufman, G. K.; Krishnamurthy, V. M.; Estroff, L. A.; Yang, J.; Whitesides, G. M. *J. Am. Chem. Soc.* **2009**, *131*, 9361−9367.
(35) Shukla, A. A.; Hubbard, B.; Tressel, T.; Guhan, S.; Low, D. *J. Chromatogr. B* **2007**, *848*, 28−39.
(36) Goodrich, J. A.; Kugel, J. F. *Binding and Kinetics for Molecular Biologists*; Laboratory Press: Cold Spring Harbor, NY, 2007.
(37) Yu, F.; Persson, B.; Lofas, S.; Knoll, W. *Anal. Chem.* **2004**, *76*, 6765−6770.
(38) Singhal, A.; Haynes, C. A.; Hansen, C. L. *Anal. Chem.* **2010**, *82*, 8671−8679.
(39) Borrebaeck, C. A. K.; Malmborg, A.-C.; Furebring, C.; Michaelsson, A.; Ward, S.; Danielsson, L.; Ohlin, M. *Nat. Biotechnol.* **1992**, *10*, 697−698.
(40) Srisa-Art, M.; Dyson, E. C.; deMello, A. J.; Edel, J. B. *Anal. Chem.* **2008**, *80*, 7063−7067.
(41) Katsamba, P. S.; Navratilova, I.; Calderon-Cacia, M.; Fan, L.; Thornton, K.; Zhu, M.; Bos, T. V.; Forte, C.; Friend, D.; Laird-Offringa, I.; Tavares, G.; Whatley, J.; Shi, E.; Widom, A.; Lindquist, K. C.; Klakamp, S.; Drake, A.; Bohmann, D.; Roell, M.; Rose, L.; Dorocke, J.; Roth, B.; Luginbuhl, B.; Myszka, D. G. *Anal. Biochem.* **2006**, *352*, 208−221.
(42) Wang, H.; Wang, Z.; Lu, M.; Zou, H. *Anal. Chem.* **2008**, *80*, 2993−2999.
(43) Myszka, D. G. In *Methods in Enzymology*, Michael, L., Johnson, G. K. A., Eds.; Academic Press, 2000; pp 325−340.
(44) Asish Xavier, K.; Willson, R. C. *Biophys. J.* **1998**, *74*, 2036−2045.
(45) Schreiber, G.; Fersht, A. R. *J. Mol. Biol.* **1995**, *248*, 478−486.
(46) Dejaegere, A.; Choulier, L.; Lafont, V.; De Genst, E.; Altschuh, D. *Biochem* **2005**, *44*, 14409−14418.
(47) Wang, Y.; Brunsen, A.; Jonas, U.; Dostálek, J.; Knoll, W. *Anal. Chem.* **2009**, *81*, 9625−9632.
(48) Seifar, R. M.; Cool, R. H.; Quax, W. J.; Bischoff, R. *Electrophoresis* **2004**, *25*, 1561−1568.
(49) Hughes, A. J.; Herr, A. E. *Proc. Natl. Acad. Sci. U.S.A.* **2012**, *109*, 21450−21455.
(50) van Oss, C. J. *J. Mol. Recognit.* **2003**, *16*, 177−190.